Noise correlations improve response fidelity and stimulus encoding

Jon Cafaro and Fred Rieke

Supplementary Material

Correlated noise simulation

This section describes the model used to illustrate the impact of noise correlations in Fig. 1. Synaptic conductances were generated and passed through an integrate-and-fire model. Modeled conductances consisted of a signal component repeated during each trial and a randomized noise component. Noise in excitatory and inhibitory conductances either originated from a common source, yielding noise correlations, or from independent sources [1]. The variance of the noise in the input conductances was held constant regardless of the noise source. Signal and noise components were generated from normal distributions, summed and convolved with either an excitatory or inhibitory synaptic filter to approximate the time course of measured synaptic inputs. Both conductances were then passed through a thresholding nonlinearity to produce the final simulated conductances. Synaptic current *I(t)* and voltage output *V(t)* were calculated as

$$I(t) = G_{exc}(t) * (V(t-\Delta t) - E_{exc}) + G_{inh}(t) * (V(t-\Delta t) - E_{inh}) \quad (1.1)$$

$$V(t) = V(t-\Delta t) + \Delta t \times I(t)/C \quad (1.2)$$

where G_{exc} and G_{inh} are the conductance waveforms, E_{exc} *and* E_{inh} are reversal potentials, and C is the cell capacitance. Voltages above a threshold were labeled as spikes after which both an absolute and relative refractory period were implemented. We did not conduct an exhaustive search of the parameters but the results of the simulation illustrated in Fig. 1 were quite robust.

Estimation of synaptic receptor steady state time constant

To estimate the time course of the change in voltage at the synaptic receptors during simultaneous conductance recordings, we analyzed midget ganglion cell responses during blockade of inhibitory synaptic input (10 μM gabazine and 1 μM strychnine). Under these conditions the variance of the current at the assumed excitatory reversal potential (E_{exc}) becomes small compared to the variance at the assumed inhibitory reversal potential (E_{inh}; Fig. S1). The large variance seen while holding at E_{inh} reflects the

variability in the excitatory conductance while the low variance at E_{exc} reflects a decrease in the driving force on the excitatory conductance. Thus, as the voltage changes from E_{inh} to E_{exc} the variance of current will decrease with a time course reflecting the time necessary to change the voltage at the receptors to E_{exc} (Fig. S1b). To minimize variance changes unrelated to synaptic input we subtracted the variance during constant light from the variance during modulated light (Fig. S1c). The resulting variance decayed rapidly, with an exponential time constant of 1.9 ± 0.6 ms (mean ± sem, 9 cells; Fig. S1d).

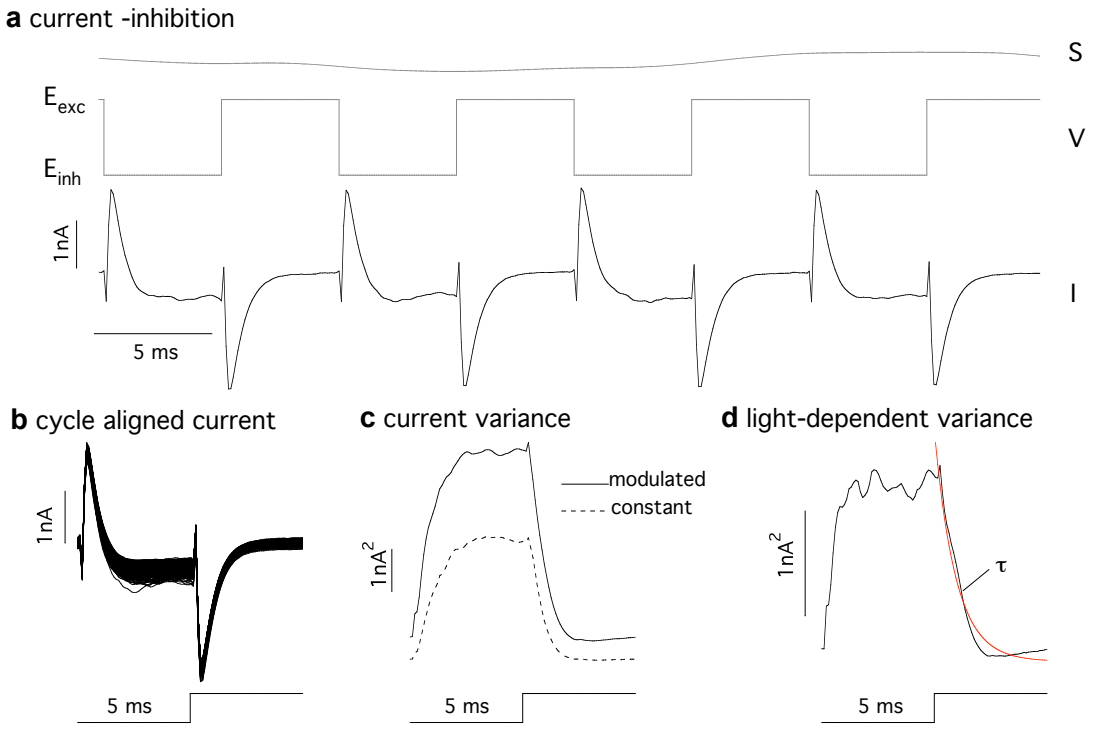

Figure S1

Time course of voltage changes at synaptic receptors. **a,** A stimulus (S) is presented during alternating voltage (V) while recording the current (I) with inhibitory synaptic input blocked (see Methods). **b,** Current responses aligned by their voltage alternation cycle. **c,** The time dependent variance of the aligned current responses during modulated and constant light. **d,** The light-dependent variance (modulated - constant) is fit with an exponential (red) and a time constant (τ) is extracted (0.5 ms in this example).

Slow drift and non-simultaneous correlations

The cross correlation of the residuals of non-simultaneous conductances often showed a small positive peak. In the midget recordings, slow drift likely accounts for most of these artifactual correlations. Slow drift in the amplitude of excitatory and inhibitory conductances over the course of the experiment could alter the amplitude of more rapidly changing conductances and thus produce artifactual rapid noise correlations [2]. This slow drift can only cause artifactual noise correlations in cases where there is consistent stimulus-dependent correlation in the excitatory and inhibitory conductances (i.e. during the modulated, but not constant, light stimulus in our experiments). The relatively modest peak of the non-simultaneous noise correlations indicates that slow drift did not dominate the noise correlations of the simultaneous conductances.

We compensated for slow drift during an experiment to determine how much it effected the measured noise correlations. Thus we calculated the residual conductances by subtracting the average of the single trials before and after the trial of interest (rather than subtracting the average of all trials) and recalculated the noise correlations. This procedure eliminated the artifactual correlations in the non-simultaneous conductances (Fig. S2) and produced a modest (12±5%) decrease in the peak of the cross correlation of the simultaneous conductances.

The same procedure reduced but did not eliminate the artifactual structure in the noise correlations for the On-Off directionally selective cells. For these cells the structure (which can be positive or negative) is likely at least in part a result of limited data. The text reports uncorrected noise correlations because the dynamic clamp experiments used measured conductances without correction for slow drift or limits of finite data.

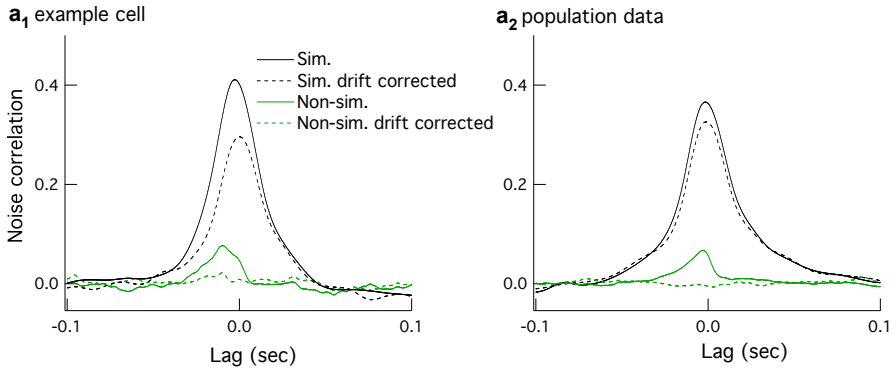

Figure S2

Noise correlations using residuals calculated from the entire data set (solid) or only surrounding trials (dashed). This figure is based on the same data as Figure 3b. **a,** The average noise correlation from an example cell. **b,** The average noise correlations from 15 midget ganglion cells.

Assessing origin and bounds of measured noise correlations

Pipette series resistance and dendritic axial resistance will distort the kinetics and amplitude of light-evoked synaptic input and cause the actual voltage at the synaptic receptors to differ from the voltage command [3]. Most importantly, using reversal potentials positive to the true excitatory reversal potential (E_{exc}) or negative to the true inhibitory reversal potential (E_{inh}) during the simultaneous conductance recordings could cause positive cross correlations even in the absence of true noise correlations. Conversely, failing to achieve the true reversal potentials will underestimate the peak amplitude of the observed noise correlation. For example, if the actual voltage at the synaptic receptors fails to reach E_{exc}, excitatory inputs will cause inward currents that in turn produce artifacts in the measured inhibitory conductances. These artifactual conductances will be anticorrelated with the excitatory conductance measured at E_{inh}. Several steps were taken to avoid and test for these possibilities.

First, our choice of cells for this work was dictated in part by their suitability for the alternating voltage approach. On-Off DSGCs and midget RGCs have relatively short dendrites (less than 100μm in On-Off DSGCs and 50μm in midget RGCs) and receive modest synaptic input compared to many other RGC types. Further, the time course of light-evoked synaptic activity is slow (50-100 ms), relaxing the constraints on rapid control of dendritic voltage. Specifically, this time constant is slow compared to the time

constant associated with voltage changes at the synaptic receptors during our recordings (see Fig. S1 and previous section).

Second, we empirically estimated the reversal potentials rather than assuming the theoretical values of 0 and -62 mV. Excitatory and inhibitory synaptic currents have slightly different time courses, creating short windows in which one or the other dominates. These brief windows permit each type of synaptic input to be monitored while manipulating the voltage command, permitting estimation of E_{exc} and E_{inh}. We used this approach conservatively so that errors would place the estimated reversal potentials between the actual ones.

To test for errors in the assumed and actual E_{inh}, we measured the cross correlation when E_{inh} was purposefully made more positive. We were able to maintain a positive cross correlation when E_{inh} was as much as 20 mV positive to the assumed and theoretical inhibitory reversal potentials. This observation makes it unlikely that the measured positive noise correlations result from assuming an E_{inh} substantially negative to the actual E_{inh}.

To test for errors in the assumed and actual E_{exc}, we suppressed inhibitory synaptic currents with gabazine (10 μM) and strychnine (1 μM). Under these conditions, the current we observe at the assumed E_{exc} will be caused by excitatory synaptic input only. If we have overshot, undershot, or estimated correctly the true E_{exc}, then we will see outward, inward, or no current, respectively. All tested cells showed inward synaptic currents at the assumed E_{exc}, indicating that our estimated E_{exc} fell short of the true E_{exc}, and hence that we underestimated the noise correlations (Fig. S3a).

Third, we used measurements with inhibitory input suppressed to estimate how much the failure to reach E_{exc} diminished the measured noise correlations. Our goal was to correct the measured cross correlation for the known error in isolating the inhibitory conductance. To make this correction we express the cross correlation between the true excitatory and inhibitory conductances, G_{exc} and G_{inh}, in terms of measured quantities: the conductances at the assumed reversal potentials, G_{exc}' and G_{inh}', and the conductance measured at the assumed E_{exc} with inhibitory input suppressed, G_b. Thus we seek a function, f, where

$$c = \frac{\langle G_{exc} \times G_{inh} \rangle}{\sqrt{\sigma_{exc}^2 * \sigma_{inh}^2}} = f(G_{exc}', G_{inh}', G_b), \tag{2.1}$$

where σ_{exc}^2 and σ_{inh}^2 are the variances of the true conductances.

We assume that $G_{exc} = G_{exc}'$ (i.e we accurately measured the excitatory conductance) and define G_{inh}' as a weighted sum of the true inhibitory conductance plus contamination from the excitatory conductance

$$G_{inh}' = d \times G_{inh} + a \times G_{exc}, \tag{2.2}$$

where a and d are scale factors determined by the current-voltage relationships of G_{exc} and G_{inh}. We determine the second term above from the current measured at the assumed E_{exc} with inhibitory input suppressed:

$$G_b = a \times G_{exc}, \tag{2.3}$$

We can also write the scale factor a as

$$a = \sqrt{\sigma_b^2 / \sigma_{exc}^2}, \tag{2.4}$$

where σ_b^2 is the variance of the conductance measured at the assumed E_{exc} during inhibitory synaptic blockade.

Substituting and rearranging we find,

$$\langle G_{exc} \times G_{inh} \rangle = \frac{\langle G_{inh}' \times G_{exc} \rangle - \langle G_b \times G_{exc} \rangle}{d}. \tag{2.5}$$

Equation 2.5 forms the numerator of the equation 2.1. To find the denominator, we calculate the variance of the true inhibitory conductance. By the definition of variance

$$\sigma_{inh'}^2 = \langle (d \times G_{inh} + a \times G_{exc})^2 \rangle - \langle d \times G_{inh} + a \times G_{exc} \rangle^2. \tag{2.6}$$

From here we can calculate the variance of the true inhibitory conductance

$$\sigma_{inh}^2 = \frac{\sigma_{inh'}^2 - a^2 \sigma_{exc}^2 + 2a\left(\langle G_{inh}' \times G_{exc} \rangle - \langle G_b \times G_{exc} \rangle\right)}{d^2}. \tag{2.7}$$

Substituting into equation 2.1, we find a function for c which depends only on G_{inh}, G_b and G_{exc},

$$c = \frac{\langle G_{inh}' \times G_{exc} \rangle - \langle G_b \times G_{exc} \rangle}{\sqrt{\left(\sigma_{inh'}^2 - a^2 \sigma_{exc}^2 + 2a\left(\langle G_{inh}' \times G_{exc} \rangle - \langle G_b \times G_{exc} \rangle\right)\right) \times \sigma_{exc}^2}}. \tag{2.8}$$

This equation estimates the cross correlation had we exactly achieved E_{exc}.

We applied equation 2.8 to five cells measured before and after suppressing inhibitory input and found that the cells with lower measured cross correlations (below 0.4) underestimated the true correlation coefficient on average by 24 ± 3% while cells with higher cross correlation coefficients underestimated the true noise correlations by only 4 ± 3% (Fig. S3b). These observations indicate that the cells we measured with higher noise correlations are likely accurate measures while cells with substantially lower measured correlations may suffer from a failure to achieve the true E_{exc}.

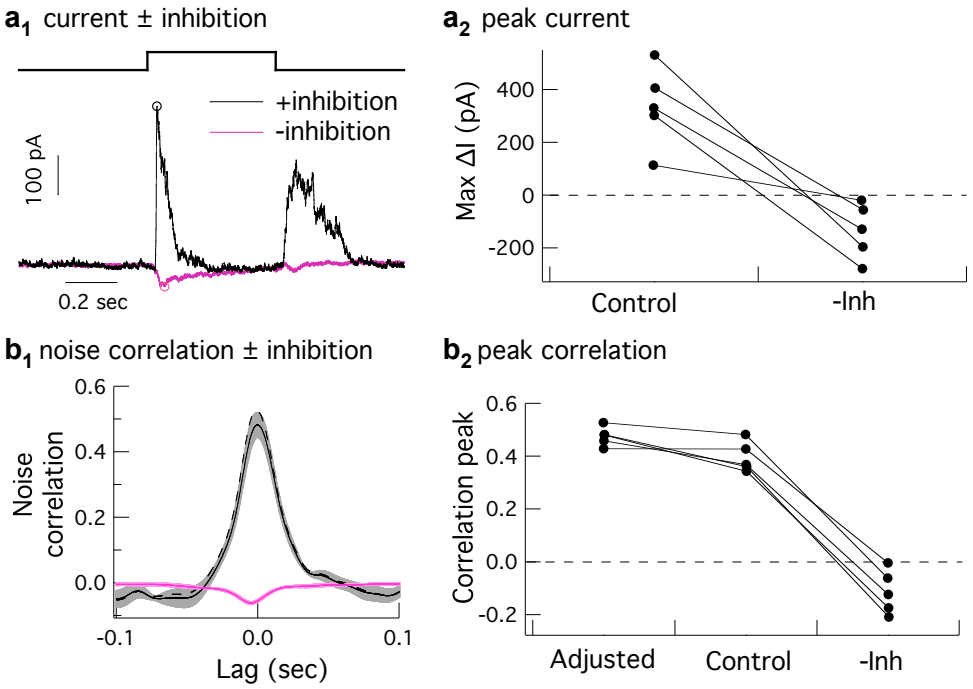

Figure S3

Test for artifactual noise correlations due to incorrect reversal potentials. **a_1,** Response of a midget RGC to a light step (gray) with the voltage held at the assumed excitatory reversal potential before (black) and during (magenta) suppression of inhibitory synaptic input. The peak current change was extracted in each condition (circles). **a_2,** Peak current changes for each cell before (Control) and during (-Inh) inhibitory synaptic blockade. **b_1,** Cross correlation (mean ± sem) of the simultaneous conductances from an example cell before (black solid) and during (magenta) inhibitory synaptic blockade. Measurements with inhibitory synaptic input suppressed permitted correction of the measured noise correlation for a known degree of contamination (dashed black line). **b_2,** Comparison of cross correlation peaks as measured normally (Control), with inhibitory input suppressed (-Inh) and when corrected for contamination (Adjusted).

Mimicking synaptic input using dynamic clamp

Dynamic-clamp experiments rely on somatic injection of synaptic inputs measured under voltage clamp. This approach will fail to mimic dendritic voltage-activated conductances that could shape synaptic inputs. Our aim in the dynamic clamp experiments was to capture key features of a cell's light response and to test the impact of noise correlations on these features. Several observations discussed below indicate that dynamic clamp experiments did this successfully.

Voltage-activated conductances could have diverse effects on synaptic integration [4]. A particular concern in On-Off DSGCs cells is the generation of dendritic spikes in response to a moving bar [5]. To check for similar dendritic spikes, we recorded current-clamp responses from several mouse On-Off DSGCs using pipettes filled with a potassium-based solution; hyperpolarizing the cells should shut down spike generation locally near the soma while still allowing for dendritic spike generation. However, unlike in rabbit cells [5], these experiements did not reveal dendritic spikelets (data no shown).

Dynamic-clamp experiments captured some but not all aspects of the cell's light-evoked spike response. Specifically, peak firing rates during dynamic clamp experiments fell short of those for light inputs. Nonetheless, dynamic-clamp responses captured the stimulus selectivity of both ganglion cell types (Fig. S4a and d) and response kinetics (Fig. S4b). Most important for this study, dynamic clamp captured the variability in the spike responses (Fig. S4c and d). The standard deviation of the light derived or the dynamic clamp derived Peri-Stimulus Time Histograms (PSTH) did not differ significantly.

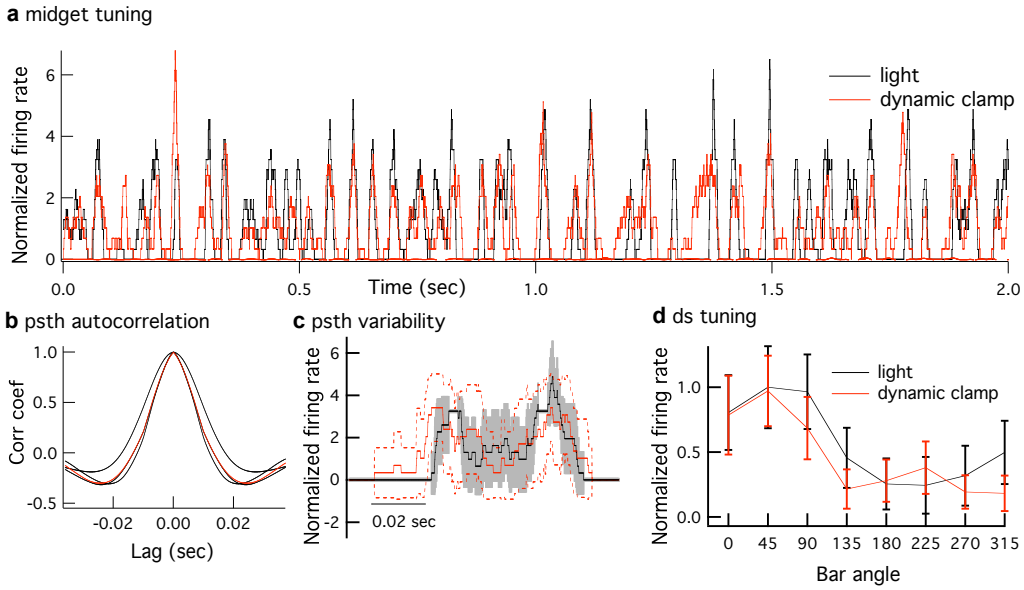

Figure S4

Comparison of light-evoked and dynamic clamp generated tuning. **a,** Comparison of Peri-Stimulus Time Histograms (PSTH) normalized by the mean firing rate from a cell attached recording (black) in a midget cell responding to a light stimuli and a different midget cell responding to conductances presented in dynamic clamp (red). The PSTH is calculated over a 10 ms sliding window. The cell attached recording is not from the same cell from which the conductances were recorded. Differences between the dynamic clamp PSTH and the light-evoked PSTH are qualitatively within the range of differences between cell attached PSTHs recorded in different cells. **b,** Autocorrelation of the PSTH from three different cell attached midget cells and a dynamic clamp cell. **c,** Enlarged portion of PSTH in panel a with error bars (mean ± s.d.). **d,** Comparison of average normalized firing rate and average standard deviation as a function of bar angle from a cell attached recording (black) in a On-Off DSGC cell responding to light and a On-Off DSGC cell responding to conductances presented in dynamic clamp (red). The cell attached recording is from the same cell from which the conductances were recorded.

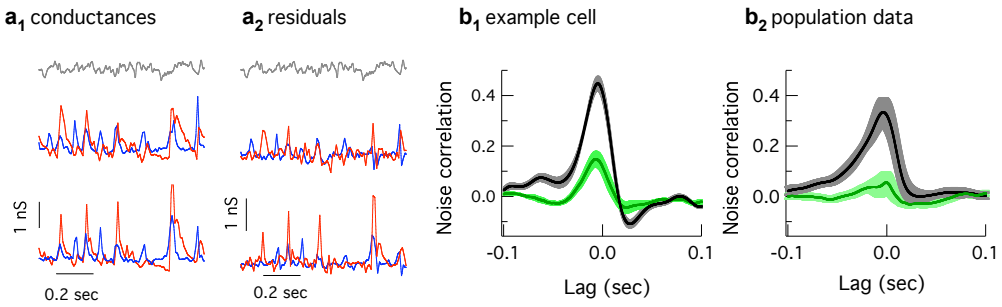

Figure S5

On-Off direction-selective RGC show strong noise correlations during full field modulated light (gray). **a_1,** Two trials of simultaneously recorded conductances. **a_2,** Residual conductances (trials from **a_1** with mean subtracted). **b_1,** Cross correlation (mean ± sem) of excitatory and inhibitory residual conductances in an example cell during simultaneous (black) and non-simultaneous recording (green). **b_2,** Cross correlation of all cells recorded (mean ± sem). Peak values ranged from 0.19 to 0.5.

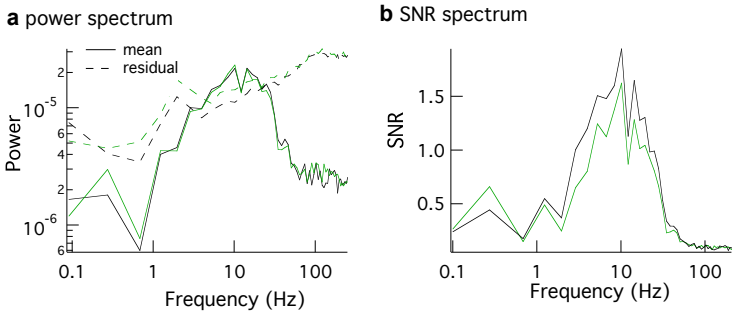

Figure S6

Calculating signal-to-noise ratio of spike trains. **a,** Power spectrum of mean (solid lines) and residual (dashed lines) spike trains during a dynamic clamp experiment with simultaneous (black) and shuffled (green) conductances. **b,** Signal-to-noise ratio of simultaneous (black) and shuffled (green) as a function of frequency.

References

1. Trong, P. K. & Rieke, F. Origin of correlated activity between parasol retinal ganglion cells. *Nat Neurosci* **11**, 1343-1351 (2008).
2. Brody, C. D. Slow covariations in neuronal resting potentials can lead to artefactually fast cross-correlations in their spike trains. *J Neurophysiol* **80**, 3345-3351 (1998).
3. Williams, S. R. & Mitchell, S. J. Direct measurement of somatic voltage clamp errors in central neurons. *Nat Neurosci* **11**, 790-798 (2008).
4. London, M. & Hausser, M. Dendritic computation. *Annu Rev Neurosci* **28**, 503-532 (2005).
5. Oesch, N., Euler, T. & Taylor, W. R. Direction-selective dendritic action potentials in rabbit retina. *Neuron* **47**, 739-750 (2005).